

AN INVESTIGATION OF THE INTERACTION BETWEEN 250–270 Mev π^+ MESONS AND CARBON NUCLEI WITH THE AID OF A PROPANE BUBBLE CHAMBER

WANG KAN-CHANG, WANG TSO-TSIANG, DING DA-TSAO, L. N. DUBROVSKII, E. N. KLADNITSKAIA, M. I. SOLOV'EV

Joint Institute for Nuclear Research

Submitted to JETP editor May 5, 1958

J. Exptl. Theoret. Phys. (U.S.S.R.) **35**, 899–906 (October, 1958)

The interaction between 250 to 270-Mev π^+ mesons and carbon nuclei was measured by means of a propane bubble chamber. The total and differential cross sections for elastic and inelastic scattering as well as the total cross section for absorption and charge exchange of the π^+ mesons were determined. The prong distributions were obtained both for stars containing mesons and for those without mesons. Within the experimental errors, elastic scattering can be described by diffractive scattering for a nucleus with $K = 0.54 \times 10^{13} \text{ cm}^{-1}$, $V = 30 \text{ Mev}$, and $R = 3.2 \times 10^{-13} \text{ cm}$. The inelastic scattering data confirm the assumption that π mesons interact with separate nucleons in the nucleus and that the number of interactions in the carbon nucleus is not large. Analysis of stars not containing mesons permits one to assert that the absorption of a π^+ meson in the carbon nucleus and the subsequent decay of the π^+ -C system cannot be explained on the basis of the evaporation model or the so-called cascade process.

1. INTRODUCTION

THERE have been many studies of π -meson interactions with nuclei, and in particular with carbon, for π meson energies below 200 Mev;¹⁻⁴ a few studies have dealt with energies greater than 200 Mev.⁵⁻⁷ These studies were made with the aid of either Wilson chambers or scintillation counters.

In the present investigation a propane bubble chamber was used to study the interactions of π^+ mesons with carbon. The advantage of using a propane bubble chamber is that the carbon nuclei are in a working fluid (C_3H_8) and the point of the π^+ -C interaction is plainly visible. The disadvantage is that the tracks left by low-energy particles are not visible. For example, elastic π^+ -C scatterings (for $E_\pi = 270 \text{ Mev}$) appear in a propane chamber as stars with a single prong.

2. EXPERIMENTAL ARRANGEMENT AND GEOMETRY

A propane bubble chamber with a diameter of 110 mm and a depth of 55 mm was used in the experiment. Its construction has already been described.⁸

The chamber was irradiated by π^+ mesons from the synchrocyclotron in the Laboratory for Nuclear Problems of the Joint Institute for Nuclear Research. Positive π mesons were generated in

a polyethylene target. In our experiments we used targets 16, 20, and 30 cm thick placed in the path of a beam of 660-Mev protons extracted from the synchrocyclotron chamber. An analyzing magnet was used to isolate a monochromatic beam of π^+ mesons from the $p + p \rightarrow \pi^+ + d$ reaction. The mesons were emitted at an angle of 9° to the direction of the proton beam. After magnetic analysis, the meson beam was sent through a collimator in a concrete shield 4 meters thick into the room containing the bubble chamber. The beam entered the chamber through a thin wall 40 mm in diameter, having first passed through a lead collimator 20 cm long and a copper filter (18 g/cm^2), both placed directly before the chamber. The filter was used to rid the π^+ -meson beam of protons with the same momentum as the mesons. The experimental set up is shown in Fig. 1. A total of 3500 photographs were obtained for π^+ mesons with an energy of $270 \pm 10 \text{ Mev}$, and 400 photographs were obtained for an energy of $250 \pm 10 \text{ Mev}$. A UIM-21 microscope⁹ was used to process the photographs.

A special electronic radio circuit, fed with 80 to 100 cps pulses from the photo-transducer of a frequency variator, was used to synchronize the operation of the bubble chamber with that of the synchrocyclotron. Every 12 seconds the circuit was opened to admit 3 or 4 pulses from the photo-

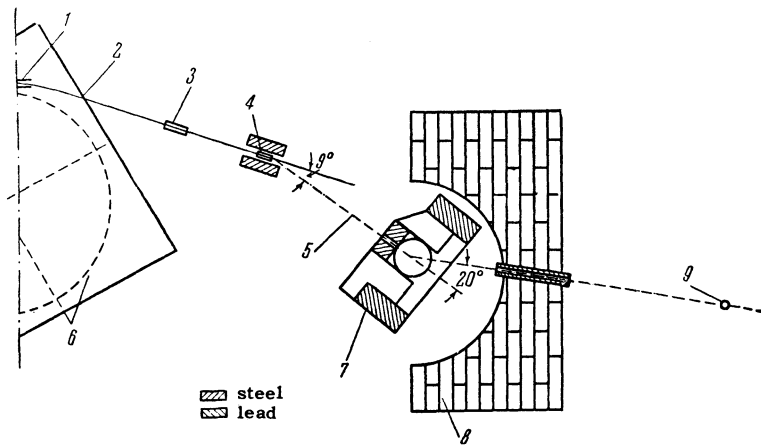


FIG. 1. The experimental setup. 1) magnetic channel, 2) proton beam with $E = 660$ Mev, 3) quadrupole lens, 4) polyethylene target, 5) π^+ meson beam, 6) synchrocyclotron chamber, 7) magnet, 8) cast-iron bricks, 9) propane bubble chamber.

transducer and accordingly to yield 3 or 4 pulses for switching on the high frequency to the control circuit. The initial triggering pulse could be regulated by a delay in such a way that the chamber would register the third or fourth pulse of the accelerated particles.

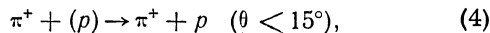
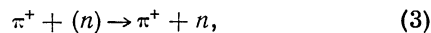
3. EXPERIMENTAL RESULTS

I. Elastic π^+ -C Scattering

The reaction



must be distinguished from other reactions such as



where (n) and (p) indicate that the reaction occurs because of a bound neutron or a bound proton respectively.

Our statistics did not include interactions by π^+ mesons with deviations larger than 10° from the beam trajectory or interactions with a scattering angle $\theta < 10^\circ$ (θ being the scattering angle of the π^+ meson in the laboratory coordinate system) For angles up to 10° large contributions are made by Coulomb scattering, π - μ -e decay, and elastic π^+ -p scattering, all of which are indistinguishable from reaction (1) in the propane chamber. Since the probability for elastic scattering of π^+ mesons by carbon for angles $> 70^\circ$ is very small, it was assumed that scattering into angles $> 70^\circ$ belonged to reaction (3).

Occurrences of elastic π^+ -p scattering in the interval $10^\circ < \theta < 15^\circ$ were excluded from the statistics in accordance with the data of Pontecorvo et al.¹⁰ Furthermore, occurrences belonging to reactions (3) and (4) for $10^\circ < \theta < 70^\circ$ (when $\theta > 15^\circ$ reaction (4) appears as a two-pronged star)

were excluded in accordance with the inelastic scattering distributions for carbon as obtained by Dzheleпов et al.⁵

The elastic scattering cross section for $10^\circ \leq \theta \leq 70^\circ$ was measured to be $\sigma_{\text{elas}} = (170 \pm 16)$ millibarns.

Besides the total elastic cross section, the differential cross section (Fig. 2) was obtained. According to Watson et al.,¹¹ the real part of the nuclear potential well for carbon is 30 Mev deep for $E_{\pi^+} = 270$ Mev. On the basis of the "optical model"¹² for positive pion-carbon scattering we

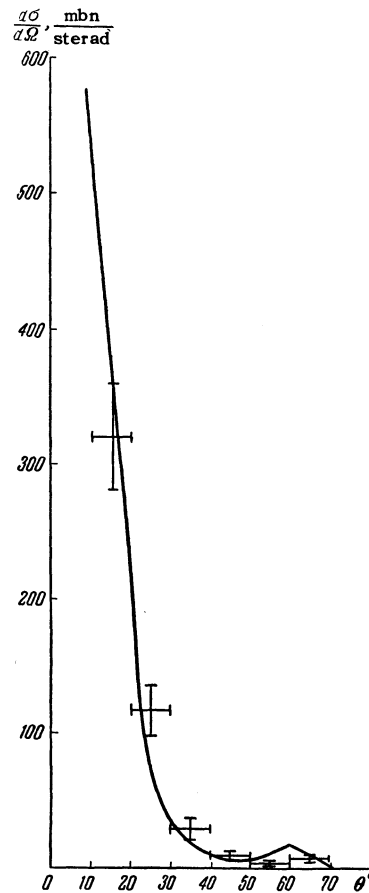


FIG. 2. Angular distribution of elastic scattering of 270-Mev π^+ mesons by carbon.

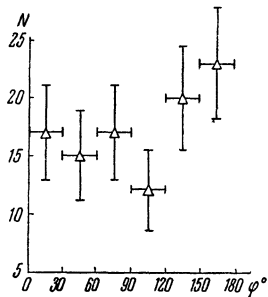


FIG. 3. The azimuthal distribution of elastic scattering of 270-Mev π^+ mesons by carbon.

computed the angular distribution for a hypothetical uniform distribution of nuclear material inside a sphere of radius $R = 1.4 A^{1/3} \times 10^{-13} \text{ cm} = 3.2 \times 10^{-13} \text{ cm}$, $K = 0.54 \times 10^{13} \text{ cm}^{-1}$ and $V = 30 \text{ Mev}$ (solid curve in Fig. 2). Here K is the absorption coefficient for π^+ mesons in the nuclear material. This coefficient was determined (cf. Dzheleпов et al.⁵) from the equation

$$K = [(\sigma_{\pi^+ - p} + \sigma_{\pi^+ - n}) A/2] / (4/3 \pi R^3),$$

where $\sigma_{\pi^+ - p}$ and $\sigma_{\pi^+ - n}$ are the total interaction cross sections for π^+ mesons with free protons and neutrons respectively for $E_\pi = 270 \text{ Mev}$, as given by Barkov and Nikol'skii,¹³ R is the radius of the carbon nucleus. The angular distribution for the elastically scattered π^+ mesons is seen to be in satisfactory agreement with the diffraction-scattering curve. The diffraction scattering cross section for $10^\circ < \theta < 70^\circ$, obtained by integrating over the theoretical curve, is 193 millibarns.

The azimuthal distribution for elastic scattering through an angle φ was also plotted for 104 cases with $15^\circ < \theta < 70^\circ$. It was found that 54 π^+ mesons were scattered into the upper hemisphere and 50 into the lower. 49 and 55 π^+ mesons were scattered respectively into the right and left hemispheres. Thus, within the limits of statistical error, the distribution in φ was symmetrical. To increase the statistics, the φ distribution was reflected about the 180° axis and folded together (Fig. 3) (i.e., points 0° and 360° coincided). It can be seen that the distribution is anisotropic. Such a distribution can be explained by the lower viewing efficiency for cases with an angle of φ near 90° , as well as by the lack of sufficient statistics.

If we add ~ 12 cases of elastic π^+ -C scattering to the $45^\circ < \varphi < 135^\circ$ interval, so that the distribution becomes isotropic, the elastic scattering cross section will be (192.2 ± 18.5) millibarns, which is in very good agreement with the diffractive scattering cross section for $V = 30 \text{ Mev}$ with $K = 0.54 \times 10^{13} \text{ cm}^{-1}$

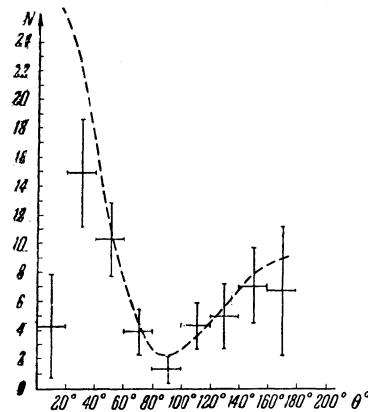
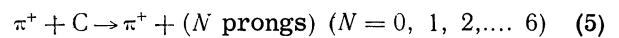


FIG. 4. The angular distribution for inelastic scattering of π mesons by carbon in the laboratory system.

II. Inelastic π^+ -C scattering

The inelastic scattering of π^+ mesons by carbon occurs as follows



It is difficult to distinguish reaction (5) from interactions that accompany π^+ meson absorption or charge exchange if the energy of the secondary π^+ meson in reaction (5) is less than 60 Mev ($g/g_0 \geq 2$ or 2.5 for π^+ mesons with $E < 60 \text{ Mev}$ and for protons with $E \leq 250 \text{ Mev}$ ¹⁴). Such ambiguous cases increased the experimental error of the measured cross section. Examples of elastic π^+ -p scattering ($\theta > 15^\circ$) are usually easily distinguished from examples of inelastic π^+ -C scattering on account of the kinematics and coplanarity of the interaction. There were, however, four cases difficult to attribute to elastic or quasi-elastic π^+ meson-proton scattering because of a considerable error in the measurement of the angle φ .

To obtain the inelastic π^+ -C cross section for $\theta > 70^\circ$ we included in our statistics of stars containing a meson those stars as described by reaction (3) that had been singled out during our investigation of one-pronged stars. It is necessary to include cases of bound nucleon scattering in the interval $0^\circ \leq \theta \leq 15^\circ$ and bound neutron scattering in the interval $15^\circ \leq \theta \leq 70^\circ$. These were obtained by comparing the angular distribution for the inelastically scattered π mesons, produced in the course of our work, with the distribution reported by Dzheleпов et al.⁵ The inelastic scattering cross section is

$$\sigma_{\text{inel}} = (120_{-19}^{+38}) \text{ millibarns.}$$

The angular distribution in the laboratory coordinate system for π^+ mesons inelastically scattered by carbon shown in Fig. 4, resembles the angular distribution for 270-Mev π^+ mesons scat-

TABLE I. Distribution of stars by prongs

Number of stars	Number of prongs						
	1*	2*	3	4	5	6	7
With a meson	46 ⁺⁹	27 ₋₃	5	1			
Without a meson	17	45 ⁺⁸	35	14	2	1	1

*Error due to distribution.

tered by hydrogen as measured by us and shown dotted in the same figure. This experimentally-determined fact indicates that scattering in the nucleus involves separate nucleons and that the number of scatterings in the carbon nucleus is small. This view has been advanced before by several authors.^{3,5,15-17} The discrepancy for $0^\circ < \theta < 20^\circ$ can be explained by assuming that when the scattering is through a small angle (in the case of a single collision), the π^+ meson loses but a small portion of its energy, while the low-energy recoil proton ($E_p < 10$ Mev) is invisible in propane. On the other hand, a careful scanning of some of the photographs failed to uncover any circumstance that would explain the reaction

$$\pi^+ + (n) \rightarrow \pi^0 + p \quad \text{for } \theta > 75^\circ.$$

Consequently, one is led to think that more is involved than the invisibility of low-energy protons in propane; Pauli's principle must also play a role.

Table I illustrates the dependence of the number of stars on the prong count per star with no account being taken of the scattered π^+ meson. From these data it follows that for the majority of inelastic scatterings of π^+ mesons a single recoil particle is visible — probably a proton. Many of these examples are quasi-elastic collisions. This fact, serves as an additional confirmation of the view that in most cases of inelastic scattering the π^+ -meson collides with an individual nucleon in the carbon nucleus and only once.

III. π^+ -Meson Absorption in Carbon and Charge Exchange

Propane is a poor photon detector. In our chamber the probability of pair production by photons was less than 3%. Actually, not a single pair was observed. Therefore, it was not possible to obtain separate cross sections for absorption and charge exchange. The observed cross section for stars without mesons was $\sigma = \sigma_a + \sigma_c = (165^{+34}_{-22})$ millibarns, where σ_a is the absorption cross section and σ_c the charge-exchange cross section. The uncertainty includes the statistical and distribution

correction error. The prong distribution for stars containing a meson and those lacking one is included in Table I.

For stars lacking a meson the angular distributions of secondary particles with a range of 16 mm or less and those with more than 16 mm were determined for a projection onto the photograph plane (16 mm is the range of a 30-Mev proton, 30 Mev being the upper limit of the evaporation spectrum¹⁸ of evaporated particles for nuclei with $A = 100$). An anisotropic prong distribution was found. As expected, the angular distribution for long (> 16 mm) prongs tended more in the forward direction. The fact that the distribution for short (< 16 mm) prongs is anisotropic and that the number of the nucleons in the carbon nucleus is small suggests that evaporation is not the mechanism of particle emission when a 270 Mev π^+ meson is absorbed by carbon. Moreover, as Table I indicates, among all the stars lacking a meson, we observed one seven-pronged star, one six-pronged star, and two five-pronged stars. The prongs of each of these stars emerge from the nucleus more or less symmetrically. For example, in the case of the six-pronged star three of the prongs extend out for more than 5 cm, and form included angles of 110° , 123° , and 118° , whereas the other three prongs extend for several millimeters. The angle between the direction of one of the high-energy prongs and the plane containing the two other similar prongs is $\sim 20^\circ$. The average number of visible ($E_p > 10$ Mev) prongs per star for all of the stars lacking a meson is 2.6. In view of the small charge of the carbon nucleus, it is possible to rule out as a mechanism the so-called cascade process, in which the number of prongs is normally much lower than the number of nuclear protons.

We propose that when π^+ mesons are absorbed by light nuclei, such as carbon, all of the energy (in our case 410 Mev) is distributed among all of the nucleons, and an "explosion" of the nucleus immediately ensues. The probability of a given number of charged particles is found in the following manner. Let us assume that upon absorption of a π^+ meson by a carbon nucleus the system formed consists of 7 protons and 5 neutrons with an excitation energy of 410 Mev. This system disintegrates very rapidly, explosively, into several free nucleons and one nuclear fragment.

All of the allowed transitions were considered. For example, a transition in which 7 protons are emitted leaving a nuclear fragment of 5 neutrons is prohibited, a transition in which two protons or two protons and one neutron are emitted with

TABLE II

Number of stars	No. of prongs for stars without a meson						
	1	2	3	4	5	6	7
Experimental data	17	45 ⁺⁸	35	14	2	1	1
Computed data	25.2	44.5	24.7	14.3	6.1	1.6	0.4

a fragment in the form of ${}_5B^{10}$ or ${}_5B^9$ is allowed, etc.

If the average energy carried off by the fragment nucleus and the binding energy of the nucleons in the nucleus are considered, one can compute the average momentum of a nucleon escaping from the system. We further propose that the probability of any allowed transition is proportional to the third power of this average momentum. By combining the probability of the allowed transitions with the corresponding number of protons we obtain the relative weights of these transitions and, for our statistics, the expected prong distribution shown in Table II.

A comparison of the experimental and computed data indicates that the absorption of π^+ mesons by carbon and the subsequent decay occurs via the proposed mechanism.

In Fig. 5, the black dots represent the energy dependence of the σ_a/σ_{total} ratio for the carbon nucleus. The data for $E_\pi = 62$ Mev were taken from Byfield et al.¹ for $E_\pi = 125$ Mev from Kessler and Lederman,³ and for $E_\pi = 230$ Mev from Dzhelepov et al.⁵ The decrease in σ_a/σ_{total} with an increase in energy is evidence of a decrease in the contribution of π^+ -meson absorption to the nuclear interaction between mesons and carbon. The probability of π^\pm -meson absorption by two nucleons in a nucleus was computed on the assumption that a π meson with momentum $|\kappa|$ is absorbed only if the relative momentum of the two nucleons equals or exceeds $|\kappa|$ or, in other words, that the distance between the two nucleons is equal to or less than $1/|\kappa|$. For this purpose a two-nucleon function $\psi_{1,2} = \sqrt{\alpha/2\pi} e^{-\alpha r}/r$ was assumed, in which case the momentum distribution is given by

$$N(k) = \left| \int_0^\infty \psi_{1,2} e^{i\kappa r} dr \right|^2$$

The quantity α was determined from the expression $\alpha^2 \hbar^2 / M = 18$ Mev.¹⁹ The meson absorption probability for the two nucleons is

$$W_a(\kappa) \sim 4\pi \int_\kappa^\infty N(k) k^2 dk,$$

where k is the wave number of the nucleons, and

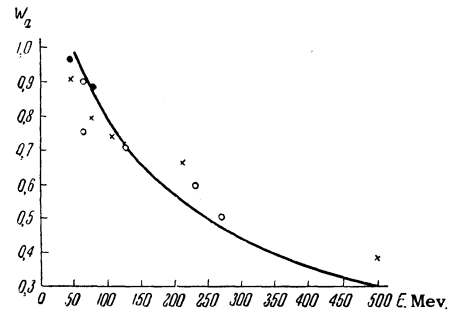


FIG. 5. The energy dependence of σ_a/σ_{total} for π mesons. \circ – interaction of π^+ mesons with carbon; \bullet – π^- meson absorption in the photographic emulsion; \times – π^+ meson absorption in emulsions.

κ the wave number of the π mesons. The energy dependence of this probability is shown by the solid curve in Fig. 5. The curve is normalized to the experimental data at $E_\pi = 125$ Mev.³ At $E_\pi = 230$ Mev⁵ and 270 Mev (the present investigation) the cross section $\sigma = \sigma_a + \sigma_c$ is known. One can then deduct the charge exchange cross section as determined from data on the charge exchange between a free proton and π^- mesons. Of course, this is approximate. As can be seen from Fig. 5, the theoretical curve reproduces the energy dependence of σ_a/σ_{total} moderately well. Experimental data on the absorption of π^+ and π^- mesons in the nuclei of the photographic emulsion²⁰⁻²³ were also included in Fig. 5. Consequently, one may conclude that the contribution of σ_a to σ_{total} decreases with an increase in energy for all the nuclei.

From Fig. 5 it can be seen that the discrepancy between the experimental and theoretical data increases as the energy of the incident π mesons increases. This can be explained by the fact that the greater the energy of the π mesons, the greater the absorption contribution from π mesons after a preliminary scattering in the nuclear matter.

4. TOTAL CROSS SECTION FOR THE INELASTIC INTERACTION OF MESONS WITH CARBON

The measured total inelastic cross section of 270-Mev π^+ mesons on carbon is

$$\sigma_{inel} = 296_{-28}^{+35} \text{ millibarns.}$$

A reduction in the distribution correction error has reduced the error here. Within the experimental error the measured cross section is in agreement with the value $\sigma_{in} = 272$ millibarns which, according to the optical model, is given by

$$\sigma_{inel} = \pi R^2 \{1 - [1 - (1 + 2KR) e^{-2KR}] / 2K^2 R^2\},$$

where R is the radius of the carbon nucleus and

is equal to 3.2×10^{-13} cm, and K is the absorption coefficient, equal to 0.54×10^{13} cm $^{-1}$. The measured cross section is also in agreement with the value of 300 millibarns as obtained from the "inelastic interaction cross section vs. energy" curve for carbon, based on the data given by Ignatenko et al.⁷

CONCLUSION

The results obtained in the present investigation of the interaction of π^+ mesons with carbon can be summarized as follows.

1. The total and differential cross sections obtained for the elastic scattering of π^+ mesons by carbon for energies from 250 to 270 Mev are in good agreement with the computations based on the optical model with an absorption coefficient $K = 0.54 \times 10^{13}$ cm $^{-1}$ and with $V = 30$ Mev and $R = 3.2 \times 10^{-13}$ cm for the real part of the complex potential.

2. For the angular distribution in φ no asymmetry was observed to the right, while to the left it was the same as reported by Kozodaev et al.²⁴

3. Within the limits of experimental error, the cross section for the inelastic interaction is in agreement with that computed from the optical model with $K = 0.54 \times 10^{13}$ cm $^{-1}$ and $R = 1.4 A^{1/3} \times 10^{-13}$ cm = 3.2×10^{-13} cm.

4. The angular distribution obtained for inelastic scattering of π^+ mesons by carbon confirms the assumption reported by other authors that the interaction of π^+ mesons with complex nuclei occurs through the interaction with separate nucleons in the nucleus and that the number of the interactions in the carbon nucleus is not large.

5. The prong distribution was obtained for stars lacking a meson. An attempt was made to explain this distribution.

6. The ratio $\sigma_a/\sigma_{\text{total}}$ was plotted as a function of π meson energy. The decrease in the ratio with an increase in meson energy is in agreement with the decrease in the probability of π meson absorption by two nucleons in the nucleus as the energy of the meson increases.

The authors express their gratitude to Prof. V. P. Dzhelepov for making it possible for them to use the accelerator belonging to the Laboratory for Nuclear Problems, to R. M. Suliaev, Iu. A. Shcherbakov, A. I. Filippov, and L. B. Parfenov for their help in conducting the experiment, and to the group of laboratory technicians under the direction of I. A. Ivanovskaia for their help in evaluating the results.

- ¹Byfield, Kessler, and Lederman, *Phys. Rev.* **86**, 17 (1952).
- ²Lederman, Byfield, Kessler and Rogers, *Phys. Rev.* **90**, 344 (A) (1953).
- ³J. Kessler and L. Lederman, *Phys. Rev.* **94**, 689 (1954).
- ⁴A. Shapiro, *Phys. Rev.* **84**, 1063 (1951).
- ⁵Dzhelepov, Ivanov, Kozodaev, Osipenkov, and Rusakov, *J. Exptl. Theoret. Phys. (U.S.S.R.)* **31**, 923 (1956), *Soviet Phys. JETP* **4**, 864 (1957).
- ⁶Ignatenko, Mukhin, Ozerov, and Pontecorvo, *Dokl. Akad. Nauk SSSR*, **103**, 395 (1955).
- ⁷Ignatenko, Mukhin, Ozerov, and Pontecorvo, *J. Exptl. Theoret. Phys. (U.S.S.R.)* **31**, 545 (1956), *Soviet Phys. JETP* **4**, 351 (1957).
- ⁸Solov'ev, Kladnitskaia, and Smirnov, *High-Energy Lab. Report* (1956).
- ⁹Kan-chang, Tso-tsiang, Da-tsao, Kladnitskaia, and Solov'ev, *High-Energy Lab. Report, Joint Institute for Nuclear Research* (November, 1957).
- ¹⁰Mukhin, Ozerov, and Pontecorvo, *J. Exptl. Theoret. Phys. (U.S.S.R.)* **31**, 371 (1956), *Soviet Phys. JETP* **4**, 237 (1957).
- ¹¹Frank, Gammel, and Watson, *Phys. Rev.* **101**, 891 (1956).
- ¹²Fernback, Serber, and Taylor, *Phys. Rev.* **75**, 1352 (1949).
- ¹³L. M. Barkov and B. A. Nilol'skii, *Usp. Fiz. Nauk.* **61**, 341 (1957).
- ¹⁴Blinov, Krestnikov, and Lomanov, *J. Exptl. Theoret. Phys. (U.S.S.R.)* **31**, 762 (1956), *Soviet Phys. JETP* **4**, 661 (1957).
- ¹⁵M. Blau and M. Caulton, *Phys. Rev.* **96**, 150 (1954).
- ¹⁶Kozodaev, Suliaev, Filippov, and Shcherbakov, *J. Exptl. Theoret. Phys. (U.S.S.R.)* **31**, 701 (1956), *Soviet Phys. JETP* **4**, 580 (1957).
- ¹⁷N. A. Mitin and E. L. Grigor'ev, *Dokl. Akad. Nauk. SSSR* **103**, 219 (1955).
- ¹⁸E. Segre, *Experimental Nuclear Physics*, vol. II, (Wiley, 1953).
- ¹⁹Bruckner, Eden, and Francis, *Phys. Rev.* **98**, 1445 (1955).
- ²⁰H. Bradner and B. Rankin, *Phys. Rev.* **87**, 547, 553 (1952).
- ²¹Bernardini, Booth and Lederman, *Phys. Rev.* **83**, 1075 (1951).
- ²²A. H. Morrish, *Phys. Rev.* **90**, 674 (1953).
- ²³G. Bernardini and F. Levy, *Phys. Rev.* **84**, 610 (1951).
- ²⁴Kozodaev, Suliaev, Shcherbakov, and Filippov, *J. Exptl. Theoret. Phys. (U.S.S.R.)* **33**, 1047 (1957), *Soviet Phys. JETP* **6**, 806 (1958).

Translated by A. Skumanich